F & S ___ revision highlighted

RUNNING TITLE

Bivalent arrangement in spermatocytes

TITLE PAGE

Chromosome size, morphology, and gene density determine bivalent positioning in metaphase I human spermatocytes

Authors*:* Laia Vergés[1], MSc., Joan Blanco[1], Ph.D., Oliver Valero[2], MSc., Francesca Vidal[1], Ph.D., and Zaida Sarrate[1], Ph.D

Addresses:

[1] Unitat de Biologia Cel·lular, Facultat de Biociències, Universitat Autònoma de Barcelona. 08193-Bellaterra (Cerdanyola del Vallès), Spain

[2] Servei d'Estadística Aplicada, Universitat Autònoma de Barcelona. 08193-Bellaterra (Cerdanyola del Vallès), Spain.

Financial support:

This study was supported by Project 2009SGR-00282 from the Generalitat de Catalunya, Spain, and Project CF-180034 from the Universitat Autònoma de Barcelona. L.V. is the recipient of a grant from the Universitat Autònoma de Barcelona (CF-180034).

Corresponding author:

Zaida Sarrate, Ph.D.

Unitat de Biologia Cel·lular, Facultat de Biociències, Universitat Autònoma de Barcelona. 08193-Bellaterra (Cerdanyola del Vallès), Spain; Tel: +34-(93)-5813733; Fax: +34-(93)-5812295. E-mail: zaida.sarrate@uab.cat

F & S ___ revision highlighted

CAPSULE

Proximity analyses of bivalents in human spermatocytes demonstrated a non-random arrangement in metaphase I influenced by chromosome size, gene density, and acrocentric chromosome morphology.

STRUCTURED ABSTRACT AND KEY WORDS

Objective: To determine if there is a preferential bivalent distribution pattern in metaphase I human spermatocytes and to analyze whether this positioning is influenced by chiasmata count, chromosome size, gene density, acrocentric morphology, and heterochromatic blocks.

Design: Proximity frequencies of bivalents were evaluated with the analysis of meiotic preparations combining sequentially standard techniques and multiplex fluorescence in situ hybridization.

Setting: Universitat Autònoma de Barcelona.

Patients: Twenty-five men consulting for fertility problems.

Interventions: Unilateral testicular biopsies.

Main Outcome Measure(s): Proximity analyses were performed for each bivalent considering as nearby bivalents those that were part of the "first ring" around the bivalent studied. Data was analyzed using Poisson regression models, multidimensional scaling (MDA), and cluster analysis.

Results: Some bivalents have a preferential relative position. Significant associations among bivalents related to chromosome size, high gene density, and acrocentric morphology were observed. Chiasmata count and heterochromatic blocks were non-conditioning parameters of the bivalent organization.

Conclusions: This study demonstrates that distribution in metaphase I is non-random and influenced by chromosome size, gene density, and acrocentric chromosome morphology.

Results support that some features defining chromosome territories are maintained during meiosis.

Keywords: bivalent, chromosome territories, meiosis, metaphase I, spermatocytes.

MANUSCRIPT

Introduction

Territorial chromosome organization is a basic feature of nuclear architecture. Chromosomes occupy what is called a chromosome territory (CT), and its location plays an important role in maintaining and regulating the genome functions (1). Currently available evidence supports the non-random arrangements of CTs, their internal architecture, and structural interactions with other CTs, and their relocation during the cell cycle and post-mitotic differentiation (2).

In the nucleus, chromosomes are distributed according to their size; the largest tend to be located in the periphery while the smallest are more central (3). Furthermore, a correlation between CT position and gene density has been proven. Chromosomes with high gene density are preferentially localized inside the nuclear area, while those that have low density are located on the periphery (1,4). Other parameters, such as activity of transcription, replication of early or late sequences of DNA, and GC content, have also been related to non-random radial nuclear arrangements of CTs and chromosomal sub-regions (2).

Configuration and maintenance mechanisms of chromosome arrangements during the cell cycle are less well understood. Some authors have concluded that no global rearrangements occur during the cell cycle and have shown robust similarities between daughter and mother cells that support the hypothesis that chromosome configuration is inheritable in mitotic cell division (5). In contrast, other authors (6) have indicated that the positioning of chromosomes is set *de novo* during interphase and that chromatin organization is not transmitted identically from the mother nucleus.

The CT neighborhood is different depending on tissue origin (7,8). Although the functional implications of the specific pattern of CT proximity for each cell-type or cell-line have not been clarified, chromosome positioning has been proposed as a common epigenetic mechanism. The contact between CTs in the interchromatin compartments leads to areas of gene-activation or -silencing, which regulate the gene expression (9).

During the last decade it has been determined that there is a non-random chromosome distribution in the sperm nucleus that has been conserved in mammalian evolution (10, 11). The relationship between chromosome positioning and functions of a sperm cell remain unknown; nevertheless, different authors have proposed some functional significance of nuclear topology. It has been suggested that the specific architecture of the sperm CTs could be important for decondensation and remodeling of chromatin domains, allowing a certain degree of epigenetic control of gene expression in the embryo (12, 13). The nuclear architecture in human sperm is also important for fertilization and early development (14). It has also been speculated that this organization influences male pronucleus development and chromosome position in the first mitotic division of the zygote (11, 13, 15).

Moreover, abnormal chromosome positioning during spermatogenesis might contribute to reproductive failures in males (13). Some studies have revealed that abnormal spermatogenesis might affect sperm chromosome positioning (16). Wiland *et al.* (17) found changes in the spatial arrangement of chromosomes in spermatozoa from reciprocal translocations carriers. Olszewska *et al.* (18) described dislocated positions of chromosomes in aneuploid spermatozoa from infertile patients. Similarly, Finch *et al.* (19) reported evidence about the relationship between altered sex chromosome positioning and male infertility.

However, we have very little knowledge of chromosome positioning during meiosis. Mudrak *et al.* (20) suggested that a non-random longitudinal chromosome order in human sperm could be constituted during meiotic stages of spermatogenesis. In the study of bivalent positioning on metaphase I (MI) spermatocytes from infertile men, Sarrate *et al.* (21) determined that bivalents 22 and 15 were observed significantly closer to the XY pair, suggesting that bivalent distribution at the metaphase plate is non-random. To extend this observation, the present study aimed to determine if there is a relative positioning pattern of bivalents on MI in human spermatocytes and to evaluate which variables might enhance this organization, including chromosome size, gene density, presence of acrocentric chromosomes, and presence of heterochromatic blocks. In addition, as synaptic anomalies have been associated with abnormal spermatogenesis (22), we also assessed whether the chiasmata count conditioned the positioning bivalent pattern.

Material and Methods

Biological samples

Testicular biopsies were obtained under local anesthesia from 25 infertile men (Spanish population) with normal karyotype. Samples were provided by assisted reproduction centers. Protocol was approved by our Institutional Review Board (IRB) and the patients gave their informed consent with regard to participation in the study. The seminal parameters of these patients are detailed in Supplemental Table I.

Chromosome preparations were obtained by processing testicular tissues following the method of Evans *et al.* (24).

Bivalent chiasmata count

Chromosome preparations were stained with Leishman (20%) (Fig. 1a, Fig. 1b) and were evaluated with an Olympus BX60 microscope (Olympus Optical España S.A., Barcelona, Spain) equipped with a capture-and-image-analysis system (CytoVision 2.7; Applied Imaging, Newcastle, UK). Coordinates of metaphases I displaying 23 well-spread bivalents were noted for further relocation and were captured to facilitate the analysis after M-FISH. Chiasmata count was recorded in all those bivalents with evaluable morphology.

Bivalent identification

Leishman-stained preparations were de-stained and processed for M-FISH (Spectra Vysion Assay, Vysis Inc.; Downers Grove, IL. USA) according to the protocol optimized in our laboratory (25) (Fig. 1c, Fig. 1d). Chromosomes appeared labeled with a combination of five different fluorochromes, obtaining 24 different color patterns, one for each chromosome. As a result, M-FISH made it possible to create a karyotype (Fig.

1e) and facilitate metaphase analysis, contrasting the images obtained after the M-FISH protocol with those previously captured after Leishman staining.

Proximity analysis

In each bivalent of every metaphase, we determined the nearby bivalents, considering "nearby" those that form the "first ring" around the studied bivalent regardless of the distance where they could be found (Fig. 1, Supplemental Table II). Proximity was studied for all the possible 253 bivalent pairs (from 23 bivalents there are $C(23,2)=1/2x23x22=253$ combinations of two without repetitions). Accordingly, nearby bivalents were noted with "1" and the absence of proximity with a "0". Data from bivalents in every metaphase I allowed us to build tables of proximity incidence for each metaphase (Supplemental Table II). Similarly, proximities between bivalent pairs were added creating a table of proximity of all the studied metaphases (Supplemental Table III).

Statistical analysis

A Poisson regression model with repeated measures (26) was established to estimate the count of nearby bivalents for each pair of bivalents. The number of metaphases observed for each patient (Supplemental Table I) was considered as an offset term of the model. The presence of over-dispersion was also taken into account. 95% confidence intervals (CI) were calculated for each pair of bivalents. In order to determine which combinations appeared with higher and lower frequency, comparisons with the overall mean CI were done.

Logistic regression models with repeated measures (27) were used to evaluate whether chiasmata count could be considered as a bivalent positioning statistically significant factor in metaphases where this data was available. Models were established for each of

the 253 bivalent pairs, considering the proximity (yes/no) as a response variable. The variable chiasmata count was recoded into three categories (less than 50 chiasmata (17MI); between 50 and 54 chiasmata (33MI); greater than 54 chiasmata (18MI)).

To evaluate if chromosome size, morphology, gene density, or the presence of heterochromatic blocks determined the bivalent organization, we established different Poisson regression models with the same methodology as described before. The studied groups were defined from the top five chromosomes of each chromosome feature: large-size chromosomes (1;2;3;4;5), small-size chromosomes (18;19;20;21;22), high-density chromosomes (11;16;17;19;22), low-density chromosomes (4;5;8;13;18), acrocentric chromosomes (13;14;15;21;22), and chromosomes with heterochromatic blocks (1;9;16). 95% confidence intervals (CI) were calculated for the bivalent pair combinations that form each group (being n= number of bivalents in a group; $n(n\text{-}1)/2!$= group combinations) and for the rest of the bivalent pairs ($253\text{-}n(n\text{-}1)/2!$).

Finally, a multidimensional scaling (MDS) analysis (28) allowed us to get a two-dimensional representation of the 23 bivalents according to their proximity. From this analysis, a reduced set of variables was obtained that was used to characterize the groups of nearby bivalents in a cluster analysis. Ward's Hierarchical Clustering Method was used (29). Results were represented in a tree dendograms using R-squared distance (30).

All resultants were obtained using software SAS v9.2 (SAS Institute Inc., Cary, NC, USA). The level of significance was set to 0.05.

Results

A full chiasmata count was only available in a total of 68MI (Supplemental Table 1). From the logistic regression models considering this variable as both quantitative and categorical, no statistically significant differences in bivalent proximities were observed among chiasmata categories. Consequently, chiasmata count was rejected as a bivalent positioning influence factor, and thus allowed us to incorporate all the metaphases in the analysis, including those in which the chiasmata count was not evaluated for every chromosome (186MI; Supplemental Table 1).

The proportions of proximity estimated by the Poisson regression models for each bivalent pair and the indication whether their confidence interval bounds were higher or lower than those of the overall mean (21.28%, IC95%=21.06–21.51%) are presented in Table 1. Twenty-two positive and eleven negative statistically significant proximities between bivalents were detected. The variables that might explain a preferential proximity between bivalent pairs were sex bivalent affinity (seven positive proximities), similar chromosome size (ten positive proximities), similar gene density (one positive proximity), and acrocentric chromosomes affinity (three positive proximities). In almost all bivalent pairs with higher proximity frequencies, we found a parameter of proximity. It has to be noted that any of these features was observed in bivalent pairs with lower proximity frequencies (Table 1).

The analysis considering the bivalent groups showed statistically significant proximities in large-size chromosomes (p=0.0022), small-size chromosomes (p=0.0462), high gene-density chromosomes (p=0.0113), and acrocentric chromosomes (p=0.0189). These groups had a statistically higher mean than the global mean, which also indicated the proximity among the bivalents form these groups (Table 2). Furthermore, we determined

the absence of preferential intragroup proximities that could have biased the results. Any bivalent pair showed statistically significant differences of proximity with respect to the other bivalent pairs of the same group, which allows us to conclude that there is a homogeny contribution of all chromosomes in the observed associations.

Results from the MDS analysis are presented in Fig. 2 and show a preferential positioning of some bivalent groups. The cluster analysis performed over the MDS factors defined three groups of bivalents according to their similarity (Fig. 2). Although cluster I (1;2;3;4;5;6;7;8;9;10;11;12) was heterogenic, cluster II (13;14;15;21;22;XY;18) showed a clear association among acrocentric chromosomes and included the XY pair, and cluster III (16;17;19;20) was formed by high density chromosomes.

Discussion

Proximity analyses on bivalent pairs revealed that some bivalents have a preferential relative position. This observation confirmed that bivalent distribution in meiotic metaphase I is non-random.

According to the results, preferential proximities between bivalents are not affected by chiasmata count variation. Since the analyzed metaphases showed a variable chiasmata count but a normal number of bivalents, this observation was expected. Indeed, it seems reasonable to suggest that if metaphases present a low chiasmata count but a normal number of bivalents, this meiotic feature does not interfere with their bivalent positioning. However, if a chiasmata decrease during metaphase leads to the presence of univalents, this situation might involve changes in bivalent positioning.

Proximity analyses also demonstrated that chromosome size conditions the spatial positioning of the bivalents during MI in agreement with studies in somatic metaphases (31, 32). Moreover, results confirmed that the size-dependence observed in the human sperm nuclei by Manvelyan *et al.* (33) is also present during MI. To explain the effect of the chromosome size in the chromosomal organization of the interphase nucleus, Sun *et al.* (3) proposed two biophysical models that could also be valid for the bivalent positioning: a volume exclusion model and a mitotic preset model. The volume exclusion model is based upon the steric hindrance caused by each chromosome size, which limits chromosome territory. Alternatively, the mitotic preset model postulates that the centromere of each chromosome is what defines its positioning in the course of mitosis.

Concerning gene density, we observed an influence of this chromosome feature in the bivalent arrangement, particularly with regard to high gene-density chromosomes. Agreeing with this observation, in sperm, gene-rich chromosomes are more frequently

observed in the interior part of the nucleus and preferably close to the apical area (21; 33). A functional role has been proposed for the influence of gene density in chromosome arrangement during meiosis.

Groups tested also showed a dependent positioning of bivalents formed by acrocentric chromosomes. Human acrocentric chromosomes present a nucleolus organizer region (NOR) in the p arm and a heterochromatin block, called a satellite. The spatial association of these bivalents could be explained because of a shared nuclear function or by the high homology of their sequences. These results are in accordance with Gurevitch *et al.* (34), who established that centromeres from acrocentric chromosomes of mature sperm have non-random arrangements. Similarly, it has already been described that acrocentric chromosomes have a predisposition to be clustered throughout the metaphase (31, 32).

Furthermore, our results showed a preferential proximity between acrocentric bivalents and the XY pair, which agrees with previous results of our group (21) and other authors that have reported the same meiotic association at the pachytene stage (35, 36). The high homology between non-centromeric heterochromatic regions of acrocentric chromosomes and Y heterochromatin chromosomes might be the reason for this association (35). Despite the proximity observed between these chromosomes, our data did not reveal a preferential proximity among chromosomes with heterochromatic blocks.

Therefore, bivalent positioning in human spermatocytes seems to be influenced by chromosome size, gene density, and presence of acrocentric chromosomes. Chromosome repositioning during spermatogenesis in porcine has been reported (11), but our results suggest that some criteria of nuclear architecture remain conserved during spermatogenesis (15, 20, 33, 34) despite possible minor changes in the chromosome positioning.

Although the analyzed samples were obtained from individuals with different seminal parameters, this variable showed no statistically significant effect in the clustering of metaphases (data not shown). For this reason, a uniform bivalent positioning among the full metaphase set was determined. The maintenance of the bivalent positioning among individuals with different etiologies supports the results in spermatozoa in which a robust pattern of nuclear organization has been described and remains unaffected by defective spermatogenesis (37).

Comentat [JBR1]: Jo aquí afegiria el test estadistic d'anàlisi-

We are aware that our approach to study the bivalent positioning has methodological limitations. To overcome the variability in the number of metaphases per patient we implemented a statistical model that modified the contribution of the patients according to the number of metaphases provided. We are conscious that one criticism of our study could be that of the analysis was performed in 2D spread metaphases. Nevertheless, due to the fact that a recurrent positioning is observed between bivalents, we believe it is accurate to consider that this result is non-random and a mirror of the real bivalent arrangement. In other words, an erroneous experimental approach would not result in a recurrent arrangement pattern consistent with the reported data. Interestingly, we validated our results performing a MDS that reinforces our findings and the experiment design used.

In conclusion, our study demonstrates that distribution in meiotic MI is non-random and influenced by chromosome size, gene density, and acrocentric chromosome morphology. Our results support the hypothesis that some features that define the chromosome territories are maintained during meiosis. The characterization of chromosome territories throughout the spermatogenic process and the analysis of chromosome positioning behavior in the presence of numerical and structural abnormalities should provide new

clues to better understand the importance of chromosome territoriality in the proper development of spermatogenesis.

Acknowledgments

The authors wish to thank the Centre de Reproducció Assistida Fecunmed (Granollers, Barcelona), Fundació Puigvert (Barcelona), Institut Marquès (Barcelona), Institut Universitari Dexeus (Barcelona) and Institut de Reproducció CEFER (Barcelona) for providing the biological samples.

References

1. Cremer T, Cremer C. Chromosome territories, nuclear architecture and gene regulation in mammalian cells. Nat Rev Genet 2001;2:292-301.
2. Cremer T, Cremer M. Chromosome territories. Cold Spring Harb Perspect Biol 2010;2:a003889.
3. Sun HB, Shen J, Yokota H. Size-dependent positioning of human chromosomes in interphase nuclei. Biophys J 2000;79:184-90.
4. Croft JA, Bridger JM, Boyle S, Perry P, Teague P, Bickmore WA. Differences in the localization and morphology of chromosomes in the human nucleus. J Cell Biol 1999;145:1119-31.
5. Gerlich D, Beaudouin J, Kalbfuss, B, Daigle N, Eils R, Ellenberg J. Global chromosome positions are transmitted through mitosis in mammalian cells. Cell 2003;112:751-64.

6. Thomson I, Gilchrist S, BickmoreWA, Chubb JR. The radial positioning of chromatin is not inherited through mitosis but is established de novo in early G1. Curr Biol 2004;14:166-72.
7. Parada LA, McQueen PG, Misteli T. Tissue-specific spatial organization of genomes. Genome Biol 2004;5:R44.
8. Zeitz MJ, Mukherjee L, Bhattacharya S, Xu J, Berezney R. A probabilistic model for the arrangement of a subset of human chromosome territories in WI38 Human fibroblasts. J Cell Physiol 2009;221:120-9.
9. Cavalli G. Chromosome kissing. Curr Opin Genet Dev 2007;17:443-50.
10. Zalenskaya IA, Zalensky AO. Non-random positioning of chromosomes in human sperm nuclei. Chromosome Res 2004;12:163-73.
11. Foster HA, Abeydeera LR, Griffin DK, Bridger JM. Non-random chromosome positioning in mammalian sperm nuclei, with migration of the sex chromosomes during late spermatogenesis. J Cell Sci 2005;118:1811-20.
12. Cremer T, Kupper K, Dietzel S, Fakan S. Higher order chromatin architecture in the cell nucleus: on the way from structure to function. Biol Cell 2004;96:555-67.
13. Zalensky AO, Zalenskaya IA. Organization of chromosomes in spermatozoa: an additional layer of epigenetic information? Biochem Soc Trans 2007;35:609-11.
14. Mudrak O, Tomilin N, Zalensky AO. Chromosome architecture in the decondensing human sperm nucleus. J Cell Sci 2005;118:41-45.
15. Hazzouri M, Rousseaux S, Mongelard F, Usson Y, Pelletier R, Faure AK *et al.* Genome organization in the human sperm nucleus studied by FISH and confocal microscopy. Mol Reprod Dev 2000;55:307-15.

16. Garagna S, Zuccotti M, Thornhill A, Fernandez-Donoso R, Berrios S, Capanna E *et al.* Alteration of nuclear architecture in male germ cells of chromosomally derived subfertile mice. J Cell Sci 2001;114:4429-34.
17. Wiland E, Zegało M, Kurpisz M. Interindividual differences and alterations in the topology of chromosomes in human sperm nuclei of fertile donors and carriers of reciprocal translocations. Chromosome Res 2008;16:291-305.
18. Olszewska M, Wiland E, Kurpisz M. Positioning of chromosome 15, 18, X and Y centromeres in sperm cells of fertile individuals and infertile patients with increased level of aneuploidy. Chromosome Res 2008;16:875-90.
19. Finch KA, Fonseka KG, Abogrein A, Ioannou D, Handyside AH, Thornhill AR, Hickson N, Griffin DK. Nuclear organisation in human sperm: preliminary evidence for altered sex chromosome centromere position in infertile males. Hum Reprod 2008;23:1263-70.
20. Mudrak O, Nazarov IB, Jones E, Zalensky AO. Positioning of chromosomes in human spermatozoa is determined by ordered centromere arrangement. PloS one 2012;7:e52944.
21. Sarrate Z, Blanco J, Vidal F. Acrocentric bivalents positioned preferentially nearby to the XY pair in metaphase I human spermatocytes. Fertil Steril 2012;98:1241-5.
22. Egozcue J, Sarrate Z, Codina-Pascual M, Egozcue S, Oliver-Bonet M, Blanco J, Navarro J, Benet J, Vidal F. Meiotic abnormalities in infertile males. Cytogenet Genome Res 2005;111:337-42.
23. World Health Organization. WHO laboratory manual for the examination of human semen and sperm-cervical mucus interaction. 4th ed. New York: Cambridge University Press, 1999.

24. Evans EP, Breckon G, Ford CE. An air-drying method for meiotic preparations from mammalian testes. Cytogenetics 1964;3:289-94.
25. Sarrate Z, Blanco J, Anton E, Egozcue S, Egozcue J, Vidal F. FISH studies of chromosome abnormalities in germ cells and its relevance in reproductive counseling. Asian J Androl 2005;7:227-36.
26. Cameron AC, Trivedi PK. Regression Analysis of Count Data. Cambridge: Cambridge University Press, 1998.
27. Agresti A. Categorical Data Analysis. 2nd ed. New Jersey: J. Wiley & Sons, 2002.
28. Cox TF and Cox MAA. Multidimensional Scaling. Chapman and Hall, 1994.
29. Anderberg MR. Cluster Analysis for Applications. New York: Academic Press, 1973.
30. Hartigan JA. Clustering Algorithms. New York: J. Wiley & Sons, 1975.
31. Mosgöller W, Leitch AR, Brown JKM, Heslop-Harrison JS. Chromosome arrangements in human fibroblasts at mitosis. Hum Genet 1991;88:27-33.
32. Wollenberg C, Kiefaber MP, Zang KD. Quantitative studies on the arrangement of human metaphase chromosomes. Hum Genet 1982;60:239-48.
33. Manvelyan M, Hunstig F, Bhatt S, Mrasek K, Pellestor F, Weise A *et al*. Chromosome distribution in human sperm – a 3D multicolor banding-study. Mol Cytogenet 2008;1:25.
34. Gurevitch M, Amiel A, Ben-Zion M, Fejgin M, Bartoov B. Acrocentric centromere organisation within the chromocenter of the human sperm nucleus. Mol Reprod Dev 2001;60:507-16.
35. Codina-Pascual M, Navarro J, Oliver-Bonet M, Kraus J, Speicher MR, Arango O, Egozcue J, Benet J. Behaviour of human heterochromatic regions during the synapsis of homologous chromosomes. Hum Reprod 2006;21:1490-7.

36. Metzler-Guillemain C, Mignon C, Depetris D, Guichaoua MR, Mattei MG. Bivalent 15 regularly associates with the sex vesicle in normal male meiosis. Chromosome Res 1999;7:369–78.

37. Ioannou D, Meershoek EJ, Christopikou D, Ellis M, Thornhill AR, Griffin DK. Nuclear organisation of sperm remains remarkably unaffected in the presence of defective spermatogenesis. Chromosome Res 2011;19:741–53.

Figure legends

Figure 1 Metaphase I in Leishman staining (A, B) and M-FISH (C, D) with the corresponding M-FISH karyotype (E). (A, C) Identification of the bivalents that constitute the first ring around the sex bivalent (indicated with an arrowhead): 4;5;9;10;12;13;21;22. (B, D) Identification of the bivalents that constitute the first ring around bivalent 21 (indicated with an arrowhead): 7;8;9;12;15;17;XY (Supplemental Table 2).

Table 1 Significantly bivalent pairs (186MI).

Sb Sex bivalent; *Cs* Chromosome size; *Gd* Gene density; *Ac* Acrocentric chromosomes

[a] Preferential bivalent proximities (+) and preferential bivalent non proximities (-)

Global mean=21.3, IC95%=21.1-21.5.

Table 2 Analysis of bivalent groups (186MI).

Global mean=21.3, IC95%=21.1-21.5.

[a] Preferential bivalent group proximity (+).

Figure 2 Multidimensional scaling analysis. (A) Two-dimensional plot of the 23 bivalents estimated from the similarity matrix (Table 2). (B) Dendogram classification of the bivalents in three clusters: I(1;2;3;4;5;6;7;8;9;10;11;12), II(13;14;15;21;22;XY;18) and III(16;17;19;20).

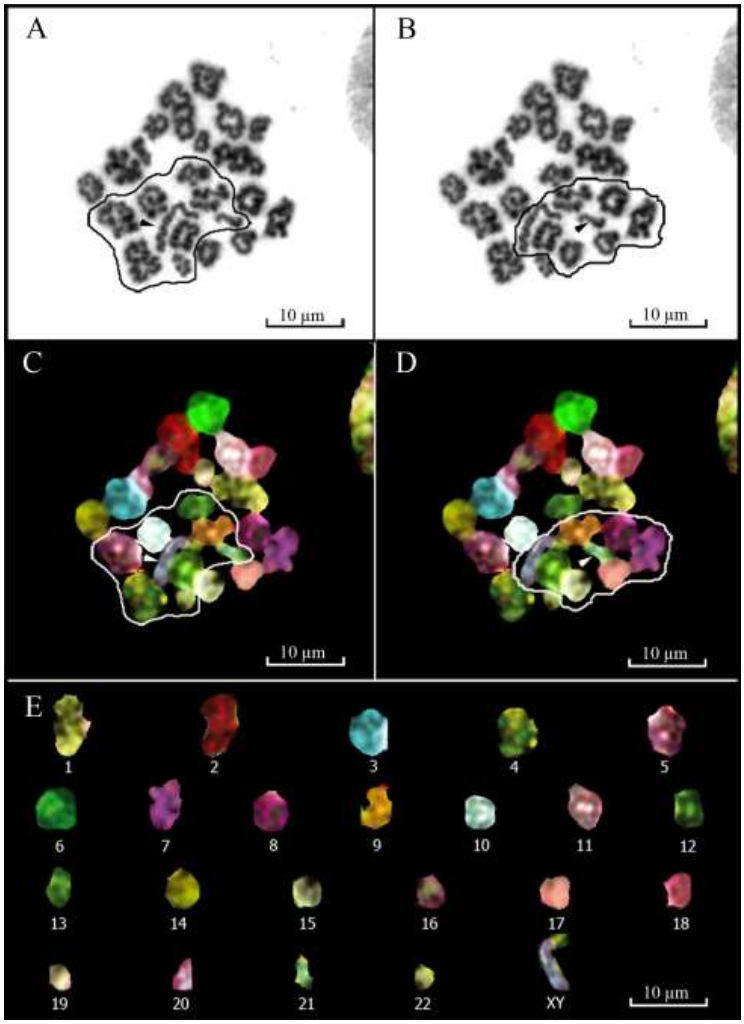
A
10 µm
B
10 µm
C
10 µm
D
10 µm
E
1
2
3
4
5
6
7
8
9
10
11
12
13
14
15
16
17
18
19
20
21
22
XY
10 µm

Figure 1

F & S ___ revision highlighted

Bivalents	Parameters				%	Confidence Limit		Proximity[a]
	Sb	Cs	Gd	Ac		Lower	Upper	
Chr22;XY	■				37	30	44	+
Chr7;XY	■				37	31	43	+
Chr15;XY	■				36	29	44	+
Chr16;17		■	■		34	29	40	+
Chr14;XY	■				32	28	37	+
Chr2;3		■			31	26	38	+
Chr13;14		■		■	31	23	40	+
Chr19;21		■			31	26	36	+
Chr1;2		■			31	26	37	+
Chr15;22				■	30	24	37	+
Chr21;22		■		■	30	25	37	+
Chr21;XY	■				30	23	37	+
Chr17;XY	■				28	22	35	+
Chr2;XY	■				28	23	35	+
Chr4;7		■			28	23	35	+
Chr9;11		■			28	23	34	+
Chr20;21		■			27	22	35	+
Chr7;16					27	23	32	+
Chr11;18					27	23	32	+
Chr16;21					27	22	33	+
Chr2;6					27	22	33	+
Chr2;5		■			26	22	31	+
Chr14;19					16	12	21	-
Chr4;13					15	11	20	-
Chr4;20					15	11	21	-
Chr6;12					15	10	21	-
Chr7;13					15	10	20	-
Chr2;20					15	10	21	-
Chr6;13					14	10	20	-
Chr2;15					13	9	20	-
Chr3;22					13	10	17	-
Chr2;21					13	10	17	-
Chr9;22					11	8	16	-

Table 1

Chromosome feature	Bivalents	%	Confidence Limit		Proximity[a]
			Lower	Upper	
Large-size chromosomes	(1;2;3;4;5)	24.0	23	25	+
Small-size chromosomes	(18;19;20;21;22)	24.7	23	27	+
High-density chromosomes	(11;16;17;19;22)	23.5	22	25	+
Low-density chromosomes	(4;5;8;13;18)	20.8	21	21	
Acrocentric chromosomes	(13;14;15;21;22)	25.0	23	27	+
Chromosomes with heterochromatic blocks	(1;9;16)	23.1	21	25	

Table 2

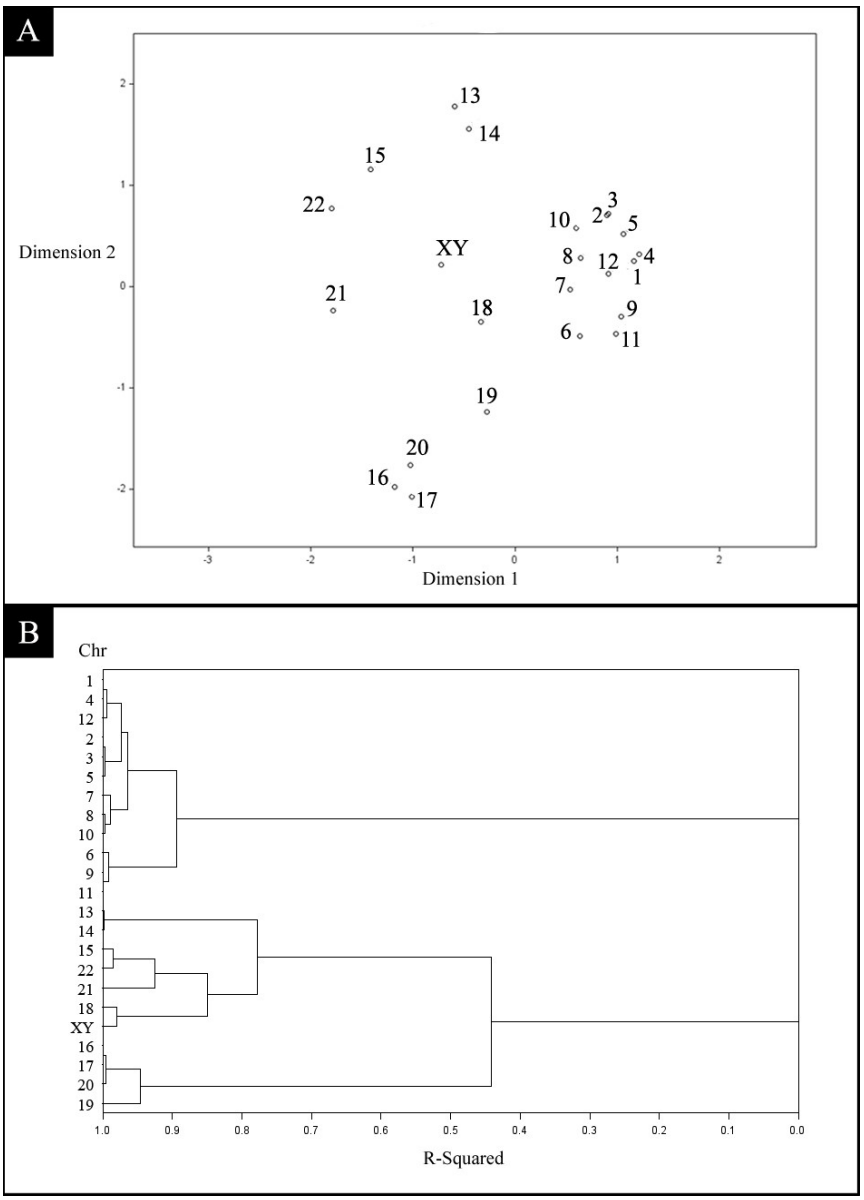
A
Dimension 2
Dimension 1
13
14
15
22
3
10
2
5
XY
8
12
4
1
7
21
18
9
6
11
19
20
16
17
B
Chr
1
4
12
2
3
5
7
8
10
6
9
11
13
14
15
22
21
18
XY
16
17
20
19
1.0
0.9
0.8
0.7
0.6
0.5
0.4
0.3
0.2
0.1
0.0
R-Squared

Figure 2